



저작자표시-비영리-변경금지 2.0 대한민국

이용자는 아래의 조건을 따르는 경우에 한하여 자유롭게

- 이 저작물을 복제, 배포, 전송, 전시, 공연 및 방송할 수 있습니다.

다음과 같은 조건을 따라야 합니다:



저작자표시. 귀하는 원저작자를 표시하여야 합니다.



비영리. 귀하는 이 저작물을 영리 목적으로 이용할 수 없습니다.



변경금지. 귀하는 이 저작물을 개작, 변형 또는 가공할 수 없습니다.

- 귀하는, 이 저작물의 재이용이나 배포의 경우, 이 저작물에 적용된 이용허락조건을 명확하게 나타내어야 합니다.
- 저작권자로부터 별도의 허가를 받으면 이러한 조건들은 적용되지 않습니다.

저작권법에 따른 이용자의 권리는 위의 내용에 의하여 영향을 받지 않습니다.

이것은 [이용허락규약\(Legal Code\)](#)을 이해하기 쉽게 요약한 것입니다.

[Disclaimer](#)

치의학박사학위논문

**Osteogenic Potential and Reaction to Human
Gingival Fibroblasts of (Y, Nb)-Zirconia**

**(Y, Nb)-지르코니아의 골형성능 및
치은세포 반응에 관한 연구**

2016년 2월

서울대학교 대학원

치의과학과 치과보철학 전공

신 지 철

Osteogenic Potential and Reaction to Human Gingival Fibroblasts of (Y, Nb)-Zirconia

지도교수 한중석

이 논문을 치의학박사학위논문으로 제출함

2015년10월

서울대학교 대학원

치 의 과학 과 치 과 보 철 학 전 공

신지철

신지철의 치의학박사 학위논문을 인준함

2015년 12월

위 원 장 이 재봉 (인)

부위원장 한 중 석 (인)

위 원 任 範 淳 (인)

위 원 李 善 炯 (인)

위 원 申 容 北 (인)

Abstract

Osteogenic Potential and Reaction to Human Gingival Fibroblasts of (Y, Nb)-Zirconia

Ji-Cheol Shin

Department of Prosthodontics

The graduate school

Seoul National University

Part I: Comparison of the osteogenic potential of titanium and modified zirconia-based bioceramics

Zirconia is now favored over titanium for use in dental implant materials because of its superior aesthetic qualities. However, zirconia is susceptible to degradation at lower temperatures. In order to address this issue, we developed modified zirconia implants that contain tantalum oxide or niobium oxide. Cells attached as efficiently to the zirconia implants as to titanium-based materials, irrespective of surface roughness. Cell proliferation on the polished surface was higher than that on the rough surfaces, but the converse was true for the osteogenic response. Cells on yttrium oxide (Y_2O_3)/tantalum oxide (Ta_2O_5)- and yttrium oxide (Y_2O_3)/niobium oxide (Nb_2O_5)-containing tetragonal zirconia polycrystals (TZP) discs ((Y, Ta)-TZP and (Y, Nb)-TZP, respectively) had a similar proliferative potential as those grown on anodized titanium. The osteogenic potential of MC3T3-E1 pre-osteoblast cells on (Y, Ta)-TZP and (Y, Nb)-TZP was similar to that of cells grown on rough-surface titanium. These data demonstrate that improved zirconia implants, which are resistant to temperature-induced degradation, retain the desirable clinical properties of structural stability

and support of an osteogenic response.

Keywords: dental implant; titanium; zirconia; LTD; osteogenic potential

Part II: Characterization of human gingival fibroblasts on zirconia surfaces containing niobium oxide

It was indicated that tetragonal zirconia polycrystal (TZP) containing yttria (Y_2O_3) and niobium oxide (Nb_2O_5) ((Y, Nb)-TZP) could be an adequate dental material to be used at esthetically important sites. The (Y, Nb)-TZP was also proved to possess its osteogenic potential comparable with those conventional dental implant material, titanium (Ti). The objective of the current study was to characterize cellular response of human gingival fibroblasts (HGFs) to smooth and rough surfaces of the (Y, Nb)-TZP disc, which were obtained by polishing and sandblasting, respectively. Various microscopic, biochemical, and molecular techniques were used to investigate the disc surfaces and cellular responses for the experimental (Y, Nb)-TZP and the comparing Ti groups. Sandblasted rough (Y, Nb)-TZP (Zir-R) discs had the highest surface roughness. HGFs cultured on polished (Y, Nb)-TZP (Zir) showed a rounded cell morphology and light spreading at 6 h after seeding and its proliferation rate significantly increased during seven days of culture compared to other surfaces. The mRNA expressions of type I collagen, integrin $\alpha 2$ and $\beta 1$ were significantly stimulated for the Zir group at 24 h after seeding. The current findings, combined with the previous results, indicate that (Y, Nb)-TZP provides appropriate surface condition for osseointegration at the fixture level and for peri-implant mucosal sealing at the abutment level producing a suitable candidate for dental implantation with an expected favorable clinical outcome.

Keywords: dental implant; zirconia; niobium; human gingival fibroblasts (HGFs); mucosal sealing

Student Number: 2001-31052

Osteogenic Potential and Reaction to Human Gingival Fibroblasts of (Y, Nb)-Zirconia

Ji-Cheol Shin, D.D.S., D.M.D., M.S.D.

Department of Prosthodontics, Graduate School, Seoul National University

(Directed by Professor **Jung-Suk Han, D.D.S., M.S., Ph.D.**)

CONTENTS

Part I: Comparison of the osteogenic potential of titanium and modified zirconia-based bioceramics

- I. Introduction
- II. Materials and Methods
- III. Results and Discussion
- IV. Conclusion
- References

Part II: Characterization of human gingival fibroblasts on zirconia surfaces containing niobium oxide

- I. Introduction
- II. Materials and Methods
- III. Results and Discussion
- IV. Conclusion
- References

Korean Abstract

Comparison of the Osteogenic Potential of Titanium and Modified Zirconia-Based Bioceramics

I. Introduction

Several types of biomaterials have been used in dental implant studies; among them, titanium has been considered the most useful, as it has excellent mechanical properties and biocompatibility [1,2]. Modification of titanium surfaces via different additive (bioactive coatings) and subtractive processes (acid etching, grit-blasting) can improve osseointegration [3-10]. Additional trials showed that incorporation of titanium into glass-based biomaterials could enhance biological responses [11,12]. However, titanium's metallic grayish color sometimes causes aesthetic problems in the anterior part of the dental implantation, as there is insufficient soft tissue to mask the peri-implant region. Furthermore, allergic reactions and sensitivities to titanium have been reported [13,14]. To minimize the soft tissue recession and aesthetic problems, many implant collars based on non-metallic materials have been developed. Tooth-colored and biocompatible ceramic materials or bioactive glass substrates are also potential candidates for novel implants [15]. Alumina is a highly biocompatible ceramic material with good aesthetic properties, but is associated with a high fracture risk. Because of this critical weakness, zirconia was introduced as a titanium alternative [16, 17]. Zirconia exists in three phases, monoclinic (M), cubic (C) and tetragonal (T), depending on temperature. M-phase is fragile at room temperature, and therefore requires stabilization to prevent tetragonal (T)-to-monoclinic (M) phase transformation in technical applications [18, 19]. A stress-induced transformation toughening mechanism improves the mechanical strength of zirconia, rendering it more suitable as a dental implant material [17,20]. Yttria

(Y₂O₃) is used as a general stabilizer for maintaining the T-phase of ZrO₂. Y₂O₃-stabilized tetragonal zirconia polycrystals (Y-TZP) have high strength, toughness, and biocompatibility, and elicit biological responses that are similar to those induced by titanium [21-23]. Therefore, Y-TZP is considered as a potential titanium alternative. However, zirconia exhibits structural instability upon low temperature degradation (LTD, often referred as "aging"), which is due to tetragonal (T)-to-monoclinic (M) phase transformation in moist or stress conditions [24]. Clearly, this limits the clinical utility of zirconia. Since the T-to-M transformation rate is most rapid at ~250 °C, it was not initially considered as a liability under physiological conditions of 37 °C [25,26]. However, several clinical failures in the use of hip prostheses were subsequently reported [25-29]. This spurred many efforts to inhibit LTD-dependent phase transformation, including addition of stabilizers such as niobium oxide (Nb₂O₅) [30,31] or tantalum oxide (Ta₂O₅) [32]. Unlike Y₂O₃, alloys of Ta₂O₅ or Nb₂O₅ contain lower numbers of cations coordinated to oxygen ions, and therefore increase the phase stability of T-ZrO₂ [30,32]. Based on these observations, we developed 3Y-TZP co-doped with Nb₂O₅ and Ta₂O₅, (Y, Nb)-TZP, and (Y, Ta)-TZP. The purpose of the present study was to evaluate the capacity of these LTD-resistant (Y, Nb)-TZP and (Y, Ta)-TZP biomaterials to support osteogenesis, with a view to using them as replacements for current titanium-based dental implant materials.

II Materials and Methods

1. Specimen Preparation

Pure titanium specimens were prepared in disc shapes (25 mm diameter and 1 mm thickness) through machining (Ti-m, Ti-machined) and treated by anodizing (Ti-a, Ti-anodizing) (OnePlant System, Warrantec Co., Ltd., Seoul, Korea). For the preparation of zirconia specimens, powders of 90.6 mol % ZrO₂, 5.3 mol % Y₂O₃, and 4.1 mol % of Nb₂O₅

were mixed for (Y, Nb)-TZP and those of 86.2 mol % ZrO₂, 7.2 mol % Y₂O₃, and 6.4 mol % Ta₂O₅ were mixed for (Y, Ta)-YZP. Disc-shaped green compacts (15 mm diameter and 1 mm thickness) were prepared by cold isostatic press of the powder mixtures at 200 MPa and then sintered for 5 h at 1650 °C in air. All zirconia discs were gradually polished and finished with diamond pastes to acquire a mirror-like surface. After polishing, (Y, Ta)-TZP and (Y,Nb)-TZP were sandblasted with 50-μm alumina (Al₂O₃) for 1 min with 1 or 2 bar pressure, respectively in order to create a rough surface.

2. Surface Roughness Assessment

The average surface roughness (R_a) and surface topography were measured using a confocal laser microscope (Carl Zeiss, Oberkochen, Germany). Surface morphology of specimens was observed using a scanning electron microscope (HITACHI S-4700 and JEOL, Tokyo, Japan) after sputter coating with platinum (Pt).

3. Cell Culture

Mouse pre-osteoblast MC3T3-E1 cells were purchased from ATCC (Manassas, VA, USA) and seeded on the discs and cultured in a-minimal essential medium (a-MEM), which contains 10% fetal bovine serum (FBS) and 1 % penicillin/streptomycin. Osteogenic media includes 10mM β-glycerophosphate and 50μg/mL ascorbic acid.

4. Cell Attachment Observation

Confocal microscopy observation was performed. Cells on the discs were fixed in 4% formaldehyde and 4',6-diamidino-2-phenylindole (DAPI, Invitrogen, Carlsbad, CA, USA) was used for detection of cell nuclei, and Alexa Fluor 568 phalloidin (Invitrogen, Carlsbad, CA, USA) was used for detection of the cytoskeleton. Fluorescence was visualized with a Carl Zeiss LSM700 microscope and analyzed with ZEN2011 software (Carl Zeiss, Oberkochen, Germany).

5. Cell Proliferation Assay

PicoGreen assay was performed using the Quant-iT PicoGreen assay kit (Invitrogen Ltd., Paisley, UK) at 1, 4, and 7 day after seeding cells on the discs. Cells were washed with PBS and lysed using TE buffer (10 mM Tris-HCl, 1 mM EDTA, pH 7.5). The DNA contents were determined by mixing 100 μ L of PicoGreen reagent and 100 μ L of DNA sample. Samples were loaded in triplicate and fluorescence intensity was measured on a GloMax-Multi Detection System machine (Promega, Madison, WI, USA). Fluorescence intensity was converted into DNA concentration with the DNA standard curve per the manufacturer's instructions. Values are represented mean \pm SD of three independent measurements.

6. Reverse-Transcription PCR and Quantitative Real-Time PCR

Cells were harvested at 3, 7, and 10 day of osteoblast differentiation and RNA was isolated using QIAzol lysis reagent (QIAGEN, Valencia, CA, USA). The Primescript RT reagent kit for reverse transcription was purchased from TAKARA (Takara Bio, Shiga, Japan). Quantitative real-time PCR was performed with the primer sets for the type I collagen gene, alkaline phosphatase (*Alp*), and osteocalcin (*Oc*) as previously described [33]. Quantitative real-time PCR was performed using Takara SYBR premix Ex Taq (Takara Bio, Shiga, Japan) on Applied Biosystems 7500 Real Time PCR system (Foster City, CA, USA). PCR primers were synthesized by Integrated DNA technology (IDT; Coralville, IA, USA). All samples were run in duplicate, and the relative levels of mRNA were normalized to those of glyceraldehyde-3-phosphate dehydrogenase (*Gapdh*).

7. Statistical Analysis

All quantitative data are presented as the mean \pm SD, each experiment was performed at least three times, and the results from one representative experiment are shown. Significant differences were analyzed using ANOVA-test. A value of $p < 0.05$ was considered statistically

significant.

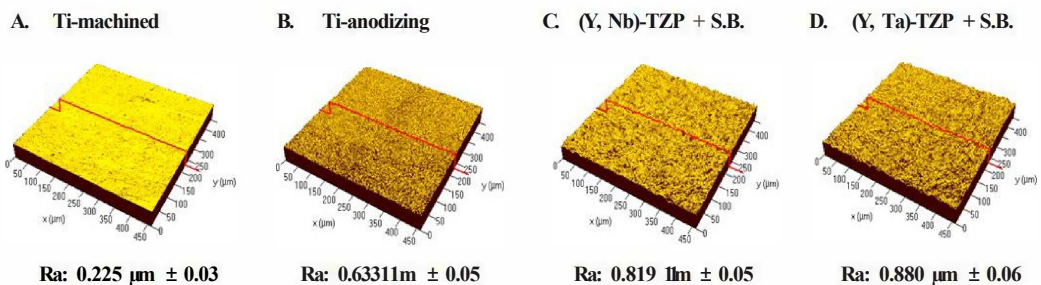
III. Results and Discussion

1. Results

1.1. Surface Analysis of the Titanium and Zirconia Discs

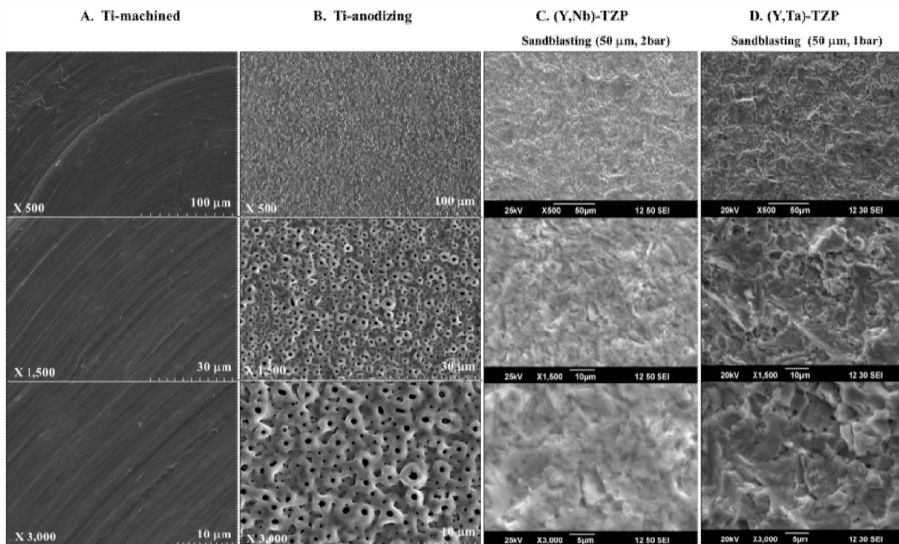
The average roughness values (R_a) of the specimens upon investigation with confocal laser microscopy are shown in Figure 1. The R_a values of Ti-m and Ti-a were $0.225 \mu\text{m} \pm 0.03$ (Figure 1A) and $0.633 \mu\text{m} \pm 0.05$ (Figure 1B), respectively. As previously reported, we increased surface roughness by modifying the surface using anodizing. The average roughness values of (Y, Nb)-TZP and (Y, Ta)-TZP were $0.092 \mu\text{m} \pm 0.001$ and $0.096 \mu\text{m} \pm 0.001$ (data not shown). To increase roughness, we sandblasted the zirconia with alumina spraying. Sandblasting with 50- μm alumina (Al_2O_3) at 1 bar pressure for 1 min created a rougher surface on the (Y, Ta)-TZP material when compared with (Y, Nb)-TZP (data not shown). To equalize the roughness, (Y, Nb)-TZP was instead subjected to 50 μm alumina (Al_2O_3) sandblasting with 2 bar for 1 min. This led to an R_a of $0.819 \mu\text{m} \pm 0.05$ for (Y, Nb)-TZP (Figure 1C) and $0.880 \mu\text{m} \pm 0.06$ for (Y, Ta)-TZP (Figure 1 D).

Figure 1. Three-dimensional confocal laser microscopy showing the roughness (R_a) of the examined substrate surfaces. (A) Titanium-machined; (B) Titanium-anodizing; (C) Sandblasted (Y, Nb)-TZP; (D) Sandblasted (Y, Ta)-TZP. (S.B.: Sandblasted).



The surface morphology of specimens was different. Machined Ti (Ti-m) has grooves because of the grinding operation (Figure 2A). After anodizing, the roughness of Ti significantly increased (Figure 2B). The surface of anodized Ti (Ti-a) was porous with patterned micrographs due to the presence of crystalline structures in the form of rutile and anatase (Figure 2B). The surface morphologies of (Y, Nb)-TZP (Figure 2C) and (Y, Ta)-TZP (Figure 2D) were similar, as each exhibited irregular rough patterns. These results were in good agreement with their average roughness (Figure 1).

Figure 2. SEM images of Titanium and Zirconia, (A) Titanium-machined; (B) Titanium-anodizing; (C) Sandblasted (Y, Nb)-TZP; (D) Sandblasted (Y, Ta)-TZP. Original magnifications are 500, 1500, and 3000x.

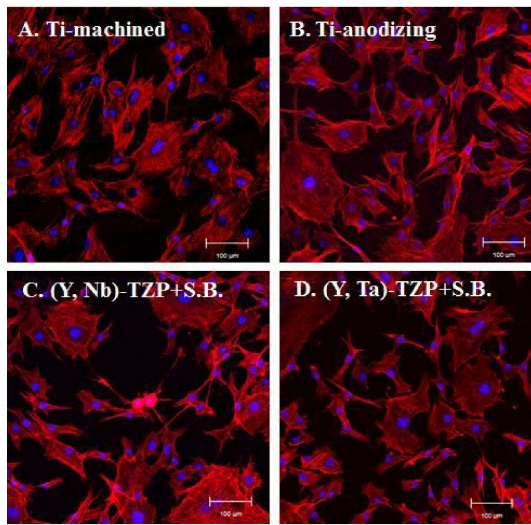


1.2. Cell Attachment and Morphology

Twenty-four hours after MC3T3-E1 pre-osteoblast cells were seeded onto the discs, cell attachment and morphology were examined using confocal laser microscopy (Figure 3). Generally, cells that adhered to the polished surface showed a regular, even size morphology (Figure 3A); however, surface roughness produced by anodizing or sandblasting induced slight morphologic irregularities and unequal cell sizes (Figure 3B-D). This appears to be due

to the surface roughness caused by uneven grooves. There was little difference in the proportion of cells with flat morphology between samples grown on titanium and those grown on zirconia, regardless of surface roughness.

Figure 3. Microscopic observation 24 h after MC3T3-E1 cells were seeded onto the Ti- or Zir-discs. (A) Titanium-machined disc; (B) Titanium-anodized disc; (C) Sandblasted (Y, Nb)-TZP disc; (D) Sandblasted (Y, Ta)-TZP disc. Original magnification is 300x and bar = 100 μ m.

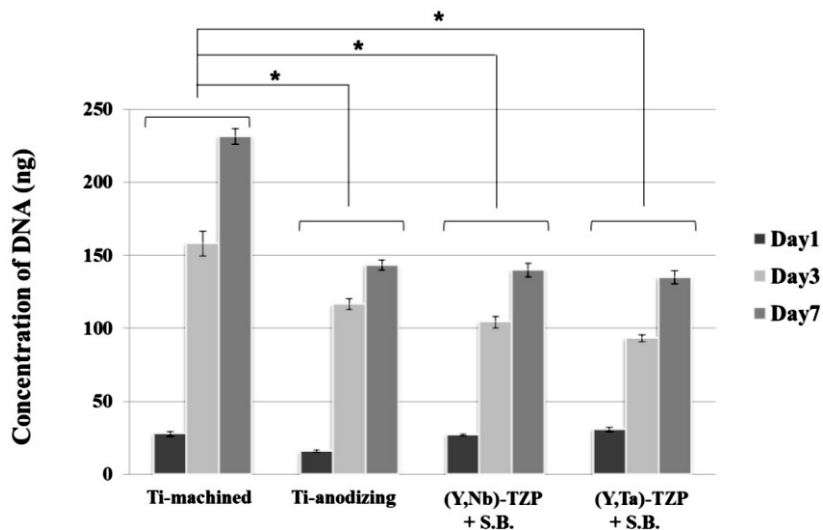


1.3. Cellular Proliferation

A PicoGreen assay was performed to examine cellular proliferation. Cells were cultured on the discs and harvested after 1, 3 and 7 day (Figure 4). The proliferation rate increased for the first 3 day, and declined thereafter. Cells on the polished surface (Ti-m) proliferated more rapidly than those on the rough surface discs (Ti-a, (Y, Nb)-TZP and (Y, Ta)-TZP), whereas there was no significant difference between cells grown on Ti-a, (Y, Nb)-TZP and (Y, Ta)-TZP. These results also indicate that the zirconia stabilizers niobium (Nb_2O_5) and tantalum (Ta_2O_5) are non-toxic to cells and that both (Y, Nb)-TZP and (Y, Ta)-TZP are biocompatible materials.

Figure 4. Cell proliferation assay (PicoGreen assay) of MC3T3-E1 cells seeded on the Ti- or Zir-discs at day 1, 3 and 7. Data are expressed as the mean \pm SD of three independent experiments. Significance was tested by one-way ANOVA test.

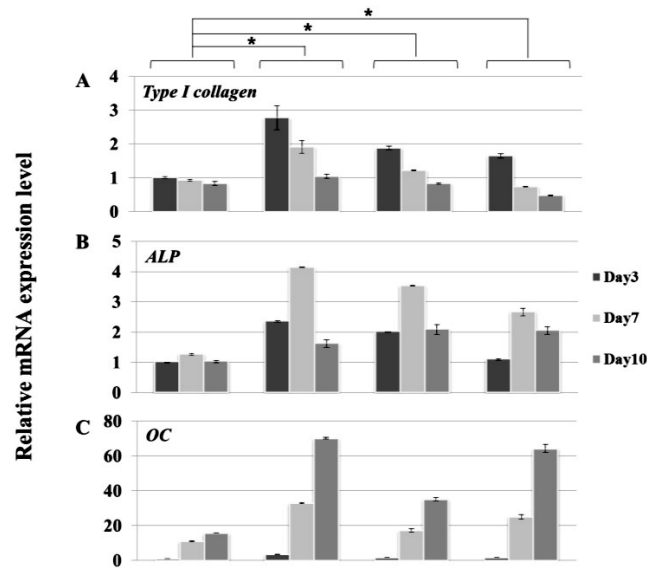
* Asterisks indicate $p < 0.05$ against the Ti-machined. (S.B.: Sandblasted).



1.4. Osteoblast Differentiation

MC3T3-E1 cells were seeded onto the discs and cultured in osteogenic media. Cells were harvested at 3, 7, and 10 day. We performed molecular profiling of osteoblast differentiation by using real-time PCR (Figure 5). The expression of osteoblast differentiation marker genes, *type I collagen* (Figure 5A), *alkaline phosphatase (Alp)* (Figure 5B), and *osteocalcin (Oc)* (Figure 5C) was consistent with the differentiation patterns we have previously described [33]. However, there was some variation in the degree of osteoblast differentiation. Cells remained largely undifferentiated on polished surface Ti-m, whereas there was greater differentiation on all the Ti-a, (Y, Nb)-TZP and (Y, Ta)-TZP rough surface discs. The expression profile of differentiation-associated markers was not significantly different between cells grown on the various rough surface discs.

Figure 5. Real-time PCR analysis of MC3T3-E1 cells grown in osteogenic media on Ti- or Zir-discs after 3, 7, and 10 day of culture. (A) Type I collagen; (B) Alkaline phosphatase (Alp); (C) Osteocalcin (Oc). Data are expressed as the mean \pm SD of three independent experiments. Significance was tested by one-way ANOVA test. * Asterisks indicate $p < 0.05$ against the Ti-machined.



2. Discussion

Biomaterials for dental implants have to meet the requirement of biocompatibility (e.g., low cellular cytotoxicity, efficient attachment, and support of proliferation and differentiation) [34]. Besides, surface topography, energy and chemical property play an important role in response of cells grown on biomaterials [35,36]. Although many reports have focused on the structural stability and strength of modified zirconia ((Y, Nb)-TZP and (Y, Ta)-TZP) [37,38], few studies have addressed whether the osteogenic response on (Y, Nb)-TZP and (Y, Ta)-TZP is different when compared to traditional titanium implants. In our study, we show that the serious limitation of LTD-dependent destabilization is compensated by addition of either

niobium (Nb_2O_5) or tantalum (Ta_2O_5). As previous studies showed that bone-to-implant surface contact was improved by increasing surface roughness [39], we opted to induce surface roughness by sandblasting with alumina particles (Al_2O_3). This process clearly enhanced increased surface roughness, as is also observed following the anodizing procedure. Although this rough surface induced cell morphological irregularities, cell attachment was equivalent between titanium and zirconia, regardless of surface roughness (Figure 3). Orsini and colleagues suggested that morphologic irregularities in sandblasted and acid-etched implants improve initial cell anchorage, thereby providing better osseointegration [40]. Similarly, our data indicated that morphologic irregularities in the rough surfaces (Ti-a, (Y, Nb)-TZP and (Y, Ta)-TZP) (Figure 3) improve the osteogenic response (Figure 5). Cellular proliferation is facilitated by polished surface material (Ti-m) (Figure 4); on the other hand, osteoblast differentiation is predominant in the rough surfaces Ti-a, (Y, Nb)-TZP and (Y, Ta)-TZP), which was confirmed by robust expression of differentiation-associated genes (Figure 5). Osteoblasts are specialized fibroblasts that secrete and mineralize the bone matrix, which contains a high proportion of type I collagen. Osteoblast differentiation proceeds through the three stages of cellular proliferation, matrix maturation, and matrix mineralization. During the initiation stage, genes that encode extracellular matrix proteins (procollagen I and fibronectin) are highly expressed. At the matrix maturation phase (around 7 day culture in the osteogenic media) alkaline phosphatase expression is at its peak, and by the beginning of matrix mineralization, genes encoding osteocalcin, bone sialoprotein, and osteopontin are expressed [33]. Based on the similar osteogenic potential and gene expression profiles we observed between titanium and modified zirconia discs, we are currently exploring strategies to enhance osteogenic potential by using zirconia implants coated with biomolecules such as the pro-osteogenic factors hydroxyapatite or BMP-2 [7,41–45].

IV. Conclusions

This *in vitro* study demonstrates that the osteogenic response of cells grown on (Y, Nb)-TZP and (Y, Ta)-TZP substrates is comparable to that observed on titanium, which is widely used in dental implant materials. By compensating the LTD weakness using stabilizers such as niobium oxide (Nb₂O₅) or tantalum oxide (Ta₂O₅), zirconia is therefore a viable substitute for titanium in terms of both structural stability and biocompatibility. Future studies are now required to determine the *in vivo* efficacy of zirconia implants with respect to osseointegration.

References

1. Adell, R.; Lekholm, U.; Rockier, B.; Branemark, P.I. A 15-year study of osseointegrated implants in the treatment of the edentulous jaw. *Int. J. Oral Surg.* **1981**, *10*, 387-416.
2. Adell, R.; Eriksson, B.; Lekholm, U.; Branemark, P.T.; Jemt, T. Long-term follow-up study of osseointegrated implants in the treatment of totally edentulous jaws. *Int. J. Oral Maxillofac. Implant.* **1990**, *5*, 347-359.
3. De Maeztu, M.A.; Braceras, I.; Aiava, J.T.; Gay-Escoda, C. Improvement of osseointegration of titanium dental implant surfaces modified with co ions: A comparative histomorphometric study in beagle dogs. *Int. J. Oral Maxillofac. Surg.* **2008**, *37*, 441-447.
4. Hsu, S.H.; Liu, B.S.; Lin, W.H.; Chiang, H.C.; Huang, S.C.; Cheng, S.S. Characterization and biocompatibility of a titanium dental implant with a laser irradiated and dual-acid etched surface. *Bio-Med. Mater. Eng.* **2007**, *17*, 53-68.
5. Knabe, C.; Howlett, C.R.; Klar, F.; Zreiqat, H. The effect of different titanium and hydroxyapatite-coated dental implant surfaces on phenotypic expression of human bone-derived cells. *J. Biomed. Mater. Res. Part A* **2004**, *71*, 98-107.
6. Knabe, C.; Klar, F.; Fitzner, R.; Radlanski, R.J.; Gross, U. *In vitro* investigation of titanium and hydroxyapatite dental implant surfaces using a rat bone marrow stromal cell culture system. *Biomaterials* **2002**, *23*, 3235-3245.
7. Le Guehennec, L.; Soueidan, A.; Layrolle, P.; Amouriq, Y. Surface treatments of titanium dental implants for rapid osseointegration. *Dent. Mater.* **2007**, *23*, 844-854.
8. Mistry, S.; Kundu, D.; Datta, S.; Basu, D. Comparison of bioactive glass coated and hydroxyapatite coated titanium dental implants in the human jaw bone. *Aust. Dent. J.*

2011, 56, 68-75.

9. Kanematu, N.; Shibata, K.I.; Kurenuma, S.; Watanabe, K.; Yamagami, A.; Nishio, Y.; Fujii, T. Cytotoxicity of oxide anodized titanium alloy evaluated by cell and organic culture study. *Gijit Shika Gakkai Zasshi* **1990**, *17*, 583-591.
10. Cunha, C.; Sprio, S.; Panseri, S.; Dapporto, M.; Marcacci, M.; Tampieri, A. High biocompatibility and improved osteogenic potential of novel ca-p/titania composite scaffolds designed for regeneration of load-bearing segmental bone defects. *J. Biomed. Mater. Res. Part A* **2013**, *101*, 1612-1619.
11. Abou Neel, E.A.; Knowles, J.C. Physical and biocompatibility studies of novel titanium dioxide doped phosphate-based glasses for bone tissue engineering applications. *J. Mater. Sci. Mater. Med.* **2008**, *19*, 377-386.
12. Kawamura, Y.; Shibata, T.; Inoue, A.; Masumoto, T. Workability of the supercooled liquid in the $Zr_{65}Al_{10}Ni_{10}Cu_{15}$ bulk metallic glass. *Acta Mater.* **1998**, *46*, 253-263.
13. Pigatto, P.D.; Guzzi, G.; Brambilla, L.; Sforza, C. Titanium allergy associated with dental implant failure. *Clin. Oral Implant. Res.* **2009**, *20*, 857.
14. Siddiqi, A.; Payne, A.G.; de Silva, R.K.; Duncan, W.J. Titanium allergy: Could it affect dental implant integration? *Clin. Oral Implant. Res.* **2011**, *22*, 673-680.
15. Kaur, G.; Pandey, O.P.; Singh, K.; Homa, D.; Scott, B.; Pickrell, G. A review of bioactive glasses: Their structure, properties, fabrication, and apatite formation. *J. Biomed. Mater. Res. Part A* **2013**, doi: 10.1002/jbm.a.34690.
16. Moller, B.; Terheyden, H.; Acil, Y.; Purcz, N.M.; Hertrampf, K.; Tabakov, A.; Behrens, E.; Wiltfang, J. A comparison of biocompatibility and osseointegration of ceramic and titanium implants: An *in vivo* and *in vitro* study. *Int. J. Oral Maxillofac. Surg.* **2012**, *41*, 638-645.
17. Nakamura, K.; Kanno, T.; Milleding, P.; Ortengren, U. Zirconia as a dental implant abutment material: A systematic review. *Int. J. Prosthodont.* **2010**, *23*, 299-309.
18. Piconi, C.; Maccauro, G. Zirconia as a ceramic biomaterial. *Biomaterials* **1999**, *20*, 1-25.
19. Kawai, Y.; Uo, M.; Wang, Y.; Kono, S.; Ohnuki, S.; Watari, F. Phase transformation of zirconia ceramics by hydrothermal degradation. *Dent. Mater. J.* **2011**, *30*, 286-292.
20. Hiromoto, S.; Tsai, A.P.; Sumita, M.; Hanawa, T. Effect of chloride ion on the anodic polarization behavior of the $Zr_{65}Al_{7.5}Ni_{10}Cu_{17.5}$ amorphous alloy in phosphate buffered solution. *Carros. Sci.* **2000**, *42*, 1651-1660.

21. Kim, D.J. Effect of Ta₂O₅, Nb₂O₅, and HfO₂ alloying on the transformability of Y₂O₃-stabilized tetragonal ZrO₂. *J. Am. Ceram. Soc.* **1990**, *73*, 115-120.
22. Sennerby, L.; Dasmah, A.; Larsson, B.; Iverhed, M. Bone tissue responses to surface-modified zirconia implants: A histomorphometric and removal torque study in the rabbit. *Clin. Implant. Dent. Relat. Res.* **2005**, *7*, S13-S20.
23. Di Carlo, F.; Prosper, L.; Ripari, F.; Scarano, A. Bone response to zirconia ceramic implants: An experimental study in rabbit. *J. Oral Implantol.* **2000**, *29*, 8-12.
24. Lughi, V.; Sergo, V. Low temperature degradation -aging- of zirconia: A critical review of the relevant aspects in dentistry. *Dent. Mater.* **2010**, *26*, 807-820.
25. Gremillard, L.; Chevalier, J. Durability of zirconia-based ceramics and composites for total hip replacement. *Key Eng. Mater.* **2008**, *361-363*, 791-794.
26. Matsui, M.; Soma, T.; Oda, I. Stress-induced transformation and plastic deformation for Y₂O₃-containing tetragonal zirconia polycrystals. *J. Am. Ceram. Soc.* **1986**, *69*, 198-202.
27. United States Food and Drug Administration. Recall of zirconia ceramic femoral heads for hip implants. *Am. Ceram. Soc. Bull.* **2001**, *80*, 14-15.
28. Masonis, J.L.; Bourne, R.B.; Ries, M.D.; McCalden, R.W.; Salehi, A.; Kelman, D.C. Zirconia femoral head fractures: A clinical and retrieval analysis. *J. Arthroplast.* **2004**, *19*, 898-905.
29. Clarke, LC.; Manaka, M.; Green, D.D.; Williams, P.; Pezzotti, G.; Kim, Y.H.; Ries, M.; Sugano, N.; Sedel, L.; Delauney, C.; *et al.* Current status of zirconia used in total hip implants. *J. Bone Jt. Surg. Am.* **2003**, *85-A*, 73-84.
30. Kim, D.J.; Jung, H.J.; Jang, J.W.; Lee, H.L. Fracture toughness, ionic conductivity, and low-temperature phase stability of tetragonal zirconia codoped with yttria and niobium oxide. *J. Am. Ceram. Soc.* **1998**, *81*, 2309-2314.
31. Ray, J.C.; Panda, A.B.; Saha, C.R.; Pramanik, P. Synthesis of niobium(v)-stabilized tetragonal zirconia nanocrystalline powders. *J. Am. Ceram. Soc.* **2003**, *86*, 514-516.
32. Ray, J.C.; Panda, A.B.; Pramanik, P. Chemical synthesis of nanocrystals of tantalum ion-doped tetragonal zirconia. *Mater. Lett.* **2002**, *53*, 145-150.
33. Cho, Y.D.; Yoon, W.J.; Woo, K.M.; Baek, J.H.; Lee, G.; Cho, .TY; Ryoo, H.M. Molecular regulation of matrix extracellular phosphoglycoprotein expression by bone morphogenetic protein-2. *J. Biol. Chem.* **2009**, *284*, 25230-25240.
34. Schmalz, G.; Arenholt-Bindslev, D. Biocompatibility of dental materials. *Dent. Clin. N.*

- Am. **2007**, *51*, 747-760.
35. Cooper, L.F. A role for surface topography in creating and maintaining bone at titanium endosseous implants. *J. Prosthet. Dent.* **2000**, *84*, 522-534.
 36. Rompen, E.; Domken, O.; Degidi, M.; Pontes, A.E.; Piattelli, A. The effect of material characteristics, of surface topography and of implant components and connections on soft tissue integration: A literature review. *Clin. Oral Implant. Res.* **2006**, *17*, 55-67.
 37. Kim, D.J.; Lee, M.H.; Lee, D.Y.; Han, J.S. Mechanical properties, phase stability, and biocompatibility of (Y,Nb)-TZP/Al2O3 composite abutments for dental implant. *J. Biomed. Mater. Res.* **2000**, *53*, 438-443.
 38. Raghavan, S.; Wang, H.; Porter, W.D.; Dinwiddie, R.B.; Mayo, M.J. Thermal properties of zirconia co-doped with trivalent and pentavalent oxides. *Acta Mater.* **2001**, *49*, 169-179.
 39. Shalabi, M.M.; Gortemaker, A.; Van't Hof, M.A.; Jansen, I.A.; Creugers, N.H. Implant surface roughness and bone healing: A systematic review. *J. Dent. Res.* **2006**, *85*, 496-500.
 40. Orsini, G.; Assenza, B.; Scarano, A.; Piattelli, M.; Piattelli, A. Surface analysis of machined *versus* sandblasted and acid-etched titanium implants. *Int. J. Oral Maxillofac. Implant.* **2000**, *15*, 779-784.
 41. Xiao, F.X.B.; Liu, R.F.; Zheng, Y.Z. Hydroxyapatite/titanium composite coating prepared by hydrothermal-electrochemical technique. *Mater. Lett.* **2005**, *59*, 1660-1664.
 42. Xiao, X.F.; Liu, R.F.; Zheng, Y.Z. Hydrothermal-electrochemical codeposited hydroxyapatite/yttria-stabilized zirconia composite coating. *J. Mater. Sci.* **2006**, *41*, 3417-3424.
 43. Jiang, Q.H.; Liu, L.; Peel, S.; Yang, G.L.; Zhao, S.F.; He, F.M. Bone response to the multilayer BMP-2 gene coated porous titanium implant surface. *Clin. Oral Implant. Res.* **2013**, *24*, 853-861.
 44. Ong, J.L.; Cardenas, H.L.; Cavin, R.; Carnes, D.L., Jr. Osteoblast responses to bmp-2-treated titanium *in vitro*. *Int. J. Oral Maxillofac. Implant.* **1997**, *12*, 649-654.
 45. Lee, B.C.; Yeo, L.S.; Kim, D.J.; Lee, J.B.; Kim, S.H.; Han, J.S. Bone formation around zirconia implants combined with rhbmp-2 gel in the canine mandible. *Clin. Oral Implant. Res.* **2013**, *24*, 1332-1338.

Characterization of Human Gingival Fibroblasts on Zirconia Surfaces Containing Niobium Oxide

I. Introduction

Implantology, a highly specialized field in dentistry, has rapidly developed the rehabilitation of dentition. Titanium (Ti) is a widely used dental implant material because of its excellent biocompatibility and strength [1]. However, its drawback of a visible metallic and grayish color in the esthetically important zone such as the anterior part of the oral cavity has necessitated developing new implant materials that have a similar color of tooth [2].

Zirconia has been introduced as an alternative material that satisfies the criteria of biocompatibility and esthetics, while the associated phenomenon of low strength by low temperature degradation (LTD) limited its clinical applications [3,4]. In a previous study, the LTD phenomenon in zirconia was substantially reduced by addition of niobium oxide (Nb_2O_5) [5,6] or tantalum oxide (Ta_2O_5) [7]. Our previous reports also proved that LTD reinforced tetragonal zirconia polycrystal (TZP) discs containing yttria (Y_2O_3) and niobium oxide (Nb_2O_5) ((Y,Nb)-TZP) have osteogenic potential similar to that of Ti [8], and that the new aerosol deposition technique for hydroxyapatite (HA) coating is significantly effective in enhancing the osteogenic potential [9].

Biocompatibility with soft tissue at the implant interface is also crucial for obtaining a successful implant system [10]. A sufficient gingival growth and mucosal sealing around the dental implant are essential to maintain the stable connection avoiding the risk of bacterial infections [11,12]. Periodontal soft tissue is mainly composed of periodontal ligament and

gingival fibroblasts [13]. Gingival fibroblasts are involved in the maintenance and production of the gingival connective tissue [14]. Poorly formed gingival connective tissue around the implant allows ease of bacterial invasion that causes inflammation resulting in marginal bone loss [15]. Hence, the formation of a tight and firm mucosal sealing between the implant and the soft tissue interface is important for a long term clinical success of the implant system [16].

We considered machined Ti the reference surface as machined is the standard implant neck and abutment surface of dental products in the market and Ti is the gold standard in implantology [17]. It has been reported that the property of collagen fibers around the implant neck area is similar *in vivo* regardless of the type of materials (Ti and Zir). Most of the collagen fibers around implants were oriented parallel and oblique-parallel to both types of implant necks. A zirconia neck seems to ensure tissue healing that is clinically and histologically comparable to that seen around a machined titanium neck. Around implants with the zirconia neck, the recorded mean probing depth, less than around implants with the machined titanium neck, is compatible with a minor inflammatory response. Zirconia showed connective tissue adhesion that was similar to that seen on the machined titanium surface, but demonstrated limited plaque formation and may provide better esthetics [18]. *In vitro* observation showed the presence of integrin subunits in human gingival fibroblasts (HGFs) and the morphological alteration of HGFs due to the surface roughness of Ti. The smooth titanium surfaces exhibited a flat monolayer of cells, while rough titanium surfaces showed cells orienting themselves along surface irregularities. It demonstrates the presence of multiple integrin subunits in human gingival fibroblasts grown in contact with titanium implant surfaces and that titanium surface roughness alters cellular morphology but appears to have limited effects on integrin expression [19]. Surface topography is an important factor in cell attachment, adhesion, proliferation, and differentiation [20], which also affects cell orientation and migration.

Cell proliferation, differentiation, protein synthesis and local factor production were affected by surface roughness. Enhanced differentiation of cells grown on rough vs. smooth surfaces for Ti surfaces was indicated by decreased proliferation and increased alkaline phosphatase and osteocalcin production. Local factor production was also enhanced on rough surfaces, supporting the contention that these cells are more differentiated [21]. However, the association between functional cellular activity and the surface roughness of materials is still controversial. In particular, opposite results have been reported about whether increasing cellular proliferation is dependent on a smooth surface of biomaterials [22,23] or not [24,25]. Thus, the objective of this study was to characterize cellular response of HGFs to smooth and rough surfaces of the (Y,Nb)-TZP disc, which were obtained by polishing and sandblasting, respectively.

II. Materials and Methods

1. Specimen Preparation

Disc shaped pure titanium specimens (25 mm diameter and 1 mm thickness) were prepared through machining (Ti-M; Ti-machined) and treated by anodizing (Ti-a; Ti-anodizing) (OnePlant System, Warrantec Co., Ltd., Seoul, Korea). Zirconia was prepared by mixing 90.6% ZrO_2 , 5.3% Y_2O_3 , and 4.1% Nb_2O_5 powders for (Y,Nb)-TZP. The compositions were selected based on the absence of low temperature degradation and reasonably high fracture toughness. Disc-shaped green compacts (15 mm diameter and 1 mm thickness) were prepared by cold isostatic pressing of the powder mixtures at 200 MPa followed by sintering for 5 h at 1650 °C in air. All zirconia discs were gradually polished and finished with diamond pastes to acquire a mirror-like surface. In order to achieve roughness similar to that of Ti-R, after polishing, the (Y,Nb)-TZP was sandblasted with 50 μm alumina (Al_2O_3) for 1 min with 2 bar pressure.

2. Surface Roughness Assessment

The average surface roughness (R_a) and surface topography were measured using a 3-D confocal laser microscope (3-D CLM; LSM700, Carl Zeiss, Oberkochen, Germany). R_a values represent the mean \pm SD of three independent experiments. Surface morphology of specimens was observed using a scanning electron microscope (Ti; HITACHI S-4700, Tokyo, Japan, Zir; SNE-4500M, SEC Co., Ltd., Suwon, Korea) after sputter coating with platinum (Pt). The surface of discs was also scanned by using an atomic force microscope (AFM; XE-100, Park Systems Inc., Seoul, Korea), and the surface roughness was calculated based on the topography of the image.

3. Cell Culture

Human gingival fibroblasts (HGFs) were purchased from American Type Culture Collection (ATCC, Manassas, VA, USA), and seeded on the discs, and cultured in Dulbecco's Modified Eagle's Medium containing 10% fetal bovine serum and 1% penicillin/streptomycin.

4. Cell Attachment Observation

Cell attachment was observed by confocal laser microscopy (CLM, Carl Zeiss, Oberkochen, Germany). Cells were fixed on the discs using 4% formaldehyde. Hoechst 33342 (Invitrogen, Carlsbad, CA, USA) was used for detecting cell nuclei, and Alexa Fluor 568 phalloidin (Invitrogen, Carlsbad, CA, USA) was used for detecting the cytoskeleton. Fluorescence was visualized with a Carl Zeiss LSM700 microscope and analyzed with ZEN2011 software (Carl Zeiss, Oberkochen, Germany).

5. Cell Proliferation Assay

Picogreen assay was performed using the Quant-iT Picogreen assay kit (Invitrogen Ltd., Paisley, UK) at one, four and seven days after seeding the cells on the discs. Cells were

washed with phosphate buffered saline (PBS) and lysed using TE buffer (10 mM Tris-HCl, 1 mM EDTA, pH 7.5). DNA concentration was determined by mixing 100 μ L of Picogreen reagent and 100 μ L of DNA sample. Samples were loaded in triplicate and fluorescence intensity was measured on a GloMax-Multi Detection System machine (Promega, Madison, WI, USA). Fluorescence intensity was converted into DNA concentration using a DNA standard curve according to manufacturer's instructions. Values are represented mean \pm SD of three independent measurements.

6. Reverse-Transcription PCR and Quantitative Real-Time PCR

Cells were harvested at 24, 48 and 72 h after seeding and RNA was isolated using QIAzol lysis reagent (QIAGEN, Valencia, CA, USA). The Primescript RT reagent kit for reverse transcription was purchased from TAKARA (Takara Bio, Shiga, Japan). Quantitative real-time PCR was performed using the primer sets for the Type I collagen, Integrin α 2, and Integrin β 1 according to [26]. Quantitative real-time PCR was performed using Takara SYBR premix Ex Taq (Takara Bio, Shiga, Japan) on Applied Biosystems 7500 Real Time PCR system (Foster City, CA, USA). PCR primers were synthesized by integrated DNA technology (IDT, Coralville, IA, USA). All samples were run in triplicate and the relative levels of mRNA were normalized to those of glyceraldehyde-3-phosphate dehydrogenase (GAPDH).

7. Statistical Analysis

All quantitative data are presented as the mean \pm SD and each experiment was performed at least three times. Results from one representative experiment are shown. Significant differences were analyzed using ANOVA-test. A value of $p < 0.05$ was considered statistically significant.

III. Results and Discussion

1. Surface Characterization of Titanium and Zirconia Discs

Proper adhesion of gingival fibroblasts to the implant surface is of importance in obtaining successful dental implantation and osseointegration [27]. Hence, surface topography is an important modulator of fibroblast adhesion [28]. As surface topography impacts cell adhesion, proliferation, and differentiation [23], the current study examined the different surface characters between Ti-machined (Ti-M), Ti-anodizing (Ti-R), (Y,Nb)-TZP (Zir) and sandblasted (Y,Nb)-TZP (Zir-R) groups. The average roughness values (R_a) and surface topography of the specimens were analyzed by three-dimensional confocal laser microscopy (3D-CLM) as shown in Figure 1A. The R_a values of Ti-M and Ti-R were $0.281 \pm 0.03 \mu\text{m}$ and $0.689 \pm 0.04 \mu\text{m}$, respectively, and those of Zir and Zir-R were $0.092 \pm 0.01 \mu\text{m}$ and $0.739 \pm 0.05 \mu\text{m}$, respectively. The R_a value of Zir was lowest due to applied fine polishing ($p < 0.05$). In order to increase the roughness to a similar level as that of titanium, sandblasting was performed with alumina particles. The conditions used for sandblasting were $50 \mu\text{m}$ alumina (Al_2O_3) at 2 bar pressure for 1 min.

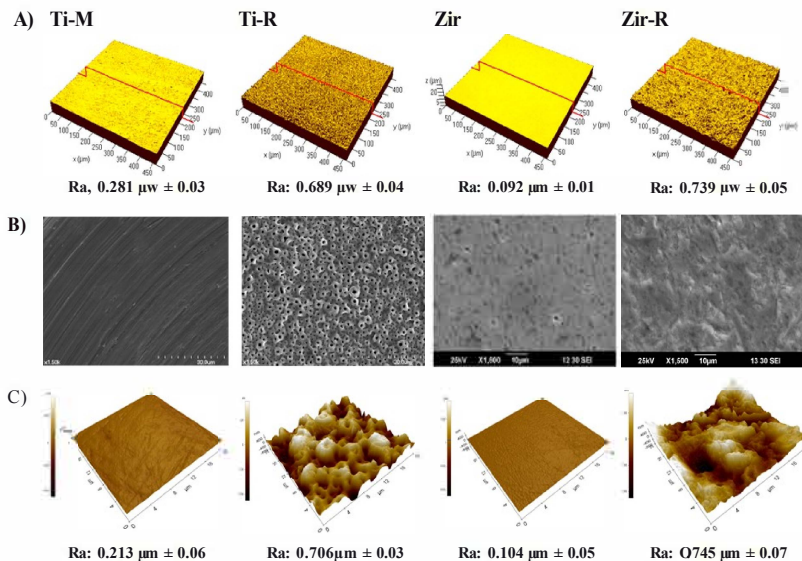


Figure 1.(A) Three-dimensional confocal laser microscopy (3D-CLM) of the examined substrate surfaces showing the roughness, R_a . **(B)** Scanning electron microscopy (SEM) images at 1500x magnification, and **(C)** atomic force microscopy (AFM) images.

Surface morphology was observed by using scanning electron microscopy (SEM) (Figure 1B). Machined Ti(Ti-M) showed regular scratches caused by mechanical machining operation, while the surface of anodized Ti (Ti-R) was porous and displayed crater like patterns owing to the presence of crystalline structures in the form of rutile and anatase. Polished mirror-like zirconia (Zir) showed a smooth and fine dotted pattern resulting from the process of sintering. However, after sandblasting with alumina, Zir-R exhibited uneven rough patterns. The atomic force microscopy (AFM) data showed in Figure 1C were in good agreement with the R_a values (Figure 1A). In respect of surface chemistry, blasting with Al_2O_3 powder may change the surface characteristics as a result of broken bonds of ZrO_2 comprising the surface, leading to surface energy higher than as-sintered one. Thus, the adhesion is prompted to lower the energy of the system. Nevertheless, the change in composition of the surface due to the blasting is likely to be negligible since the ceramic processing to produce the specimens was including the ball milling, homogeneous heat treatment at 1250 °C and the following attrition milling, is known to provide uniform distribution of components so that the composition in bulk and surface is reasonably identical.

2. Cell Attachment and Morphology

It is well established that smooth Ti surfaces favor fibroblast attachment, whereas rough Ti surfaces promote osseointegration [29,30]. In order to investigate this phenomenon between (Y,Nb)-TZP and Ti, HGFs were seeded onto the discs and harvested at 6 and 24 h, and CLM observation was followed to examine cellular attachment and morphology (Figure 2). At the early cell culture stage (6 h), cells were observed to be well attached and stretched on the Ti-Mand Ti-R compared to that on Zir or Zir-R (Figure 2A). After 24 h of cell seeding,

the state of cell morphology was somewhat similar between the Ti and Zir, regardless of their surface roughness (Figure 2B). Cells on the Zir were observed to be widely spread and elongated with good attachment. However, those on Zir-R were narrower and less stretched than Zir, probably indicating weaker binding with the surface.

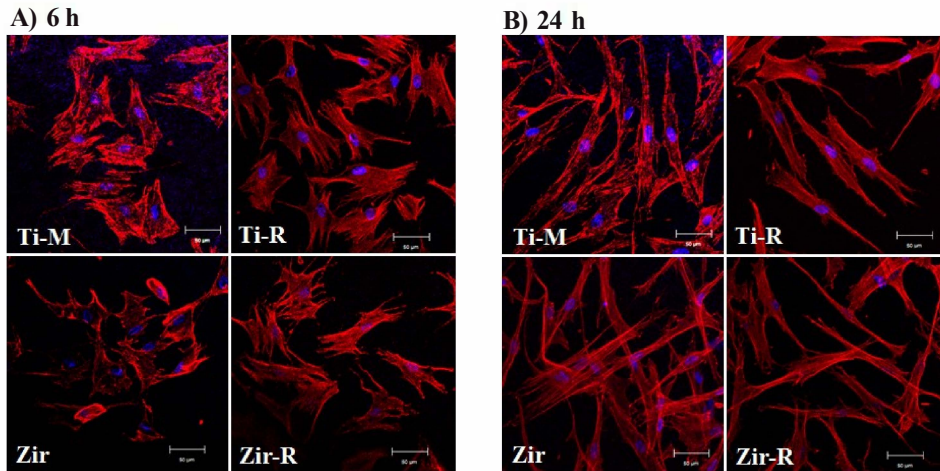


Figure 2. Microscopic observation after human gingival fibroblast (HGF) cells were seeded onto the discs at (A) 6 h and (B) 24 h. Original magnification is 300 x and scale bar = 50 μm.

3. Cell Proliferation

Cell proliferation was evaluated by the picogreen assay. For this purpose, the HGFs were seeded onto discs and cultured for one, four, and seven days (Figure 3). HGFs were observed to proliferate well in cell cultures on all types of surfaces. The proliferation rate on Zir was significantly increased at Day 4 ($p < 0.05$) and proliferation was promoted until Day 7, indicating a positive effect of surface roughness. Generally, the smooth surfaces (*i.e.*, Ti-M or Zir) induced higher cell proliferation comparison to the rough surfaces (*i.e.*, Ti-R or Zir-R). These results correlate well with those observed in case of cell attachment and morphology, which showed a more aligned and spreaded pattern in the Zir and Ti-M (Figure 2).

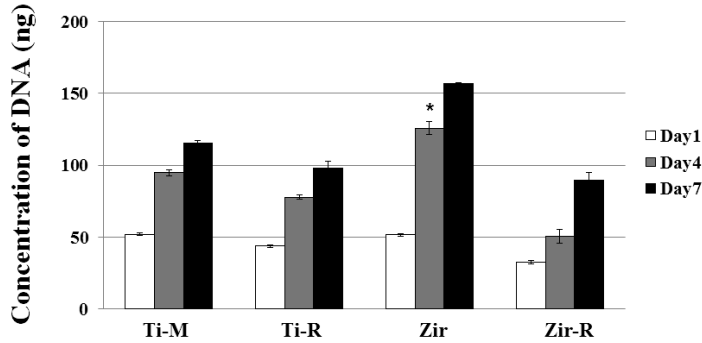


Figure 3. Cell proliferation assay (picogreen assay) of MC3T3-E1 cells at Day 1, 4 and 7 seeded on Ti- or Zir-discs. Data are expressed as the mean \pm standard deviation (SD) of three independent experiments. Significance was tested by one-way analysis of variance (ANOVA) test (* $p < 0.05$).

4. Cell Differentiation

Quantitative real time polymerase chain reaction (RT-PCR) was performed to evaluate the mRNA expression level of collagen and integrin subunits. HGFs were seeded onto discs and cultured for 24, 48 and 72 h to analyze mRNA expression levels of Type I collagen, Integrin $\alpha 2$, Integrin $\beta 1$ (Figure 4). Collagen I is mainly produced in the gingival fibroblasts, osteoblasts and periodontal ligament [31,32]. It is an important factor of gingival connective tissue and contributes to rapid periodontal tissue regeneration and maintenance of tissue architecture [33,34]. In this experiment, the mRNA levels of Type I collagen were significantly high on Zir after 24 and 72 h of cell culture ($p < 0.05$). It has been well indicated that integrins, whose α and β subunits constitute non-covalently linked $\alpha\beta$ heterodimers, are responsible for cell adhesion [35]. Several integrin subunits including $\alpha 2$, $\alpha 5$, $\beta 1$ and $\beta 3$ were identified in the periodontal tissue [19,36]. Given the interplay of integrins with the extracellular matrix (ECM) and cytoskeleton [37], they regulate cellular functions, cell proliferation, adhesion, shape, and differentiation [34]. As seen in Figure 4, the mRNA levels of Integrin $\alpha 2$ and $\beta 1$ showed almost similar patterns at each of the time points. Interestingly, Zir led to significantly high mRNA

expression in Integrin $\alpha 2$ at 24 and 48 h, and Integrin $\beta 1$ at every time point ($p < 0.05$). These results indicate that the mRNA expression of integrin subunits is correlated with cellular attachment and proliferation on the smooth Zir surface, which is partly supported by some reports [26]. In our data, Type I collagen mRNA expression was high at day 1 and then decreased (Figure 4). We guess that Type I collagen protein is well produced around one day, indicating a good attachment of gingival fibroblasts on the discs, especially Zir. In the case of Zir, cell morphology was round after 6 h of seeding; however, cytoskeleton was stretched at 24 h (Figure 2). It reflects the big increase of Type I collagen mRNA expression in the Zir. Both $\alpha 1\beta 1$ and $\alpha 2\beta 1$ integrins are cell surface receptors for collagens. Among them, $\alpha 2\beta 1$ integrins have been shown to serve as specific receptors for type I collagen in fibroblasts, and acts as a positive regulator of type I collagen gene expression [38]. Based on these, we assume that Integrin $\alpha 2$ or $\beta 1$ gene expression is closely related with type I collagen gene expression as our data has shown (Figure 4). In contrast with our observations, some previous studies observed no significant differences in the mRNA expression level for integrin, collagen, and fibronectin on the different disc types (*i.e.*, grooved Zir, smooth Zir, and Ti) [39].

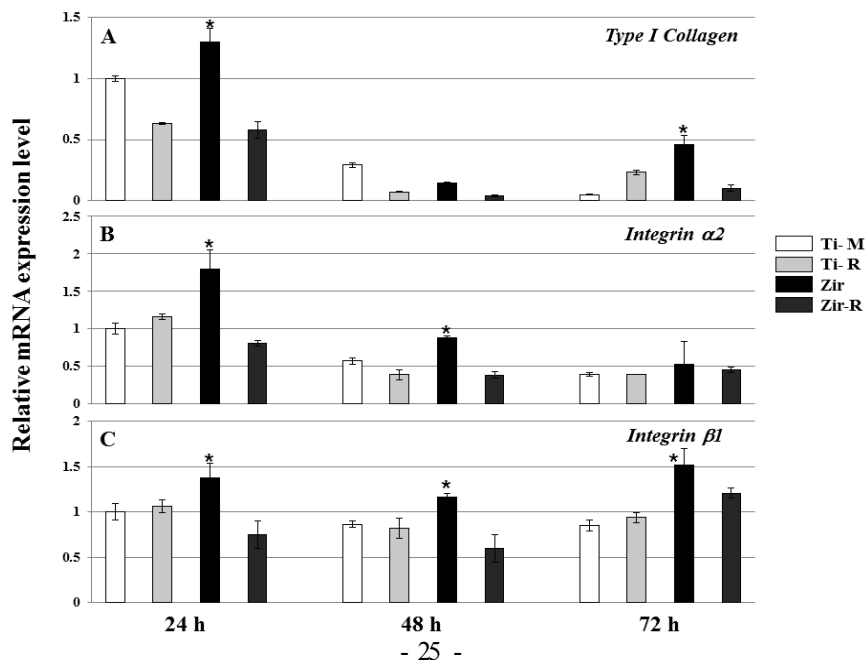


Figure 4. Real time polymerase chain reaction (RT-PCR) (A) Type I collagen, (B) Integrin $\alpha 2$, and (C) Integrin $\beta 1$ in HGFs cultured on Ti- or Zir-discs after 24, 48 and 72 h. Data are expressed as the mean \pm SD of three independent experiments. Significance was tested by one-way ANOVA test (* $p < 0.05$).

IV. Conclusions

Through the HGFs cellular response on the (Y,Nb)-TZP discs with different surface roughness, we proved that well-polished zirconia is superior to cell adhesion and proliferation showing increased type I collagen and Integrin $\alpha 2$ and $\beta 1$ expression level. In comparison with Ti, zirconia shows similar cellular response in the late phase of cell culture. Based on our previous [8,9] and present data, we conclude that appropriate surface roughness of (Y,Nb)-TZP is important; rough surface for the osseointegration at the fixture level and smooth surface for the peri-implant mucosal sealing at the abutment level in the dental implant application of zirconia. As our study involves *in vitro* experiments with primary HGFs, it could have limitations for explaining general phenomenon of HGFs in view of significance.

References

1. Buser, D.; Janner, S.F.; Wittneben, T.G.; Bragger, U.; Ramseier, C.A.; Salvi, G.E. 10-year survival and success rates of 511 titanium implants with a sandblasted and acid-etched surface: A retrospective study in 303 partially edentulous patients. *Clin. Implant Dent. Relat. Res.* **2012**, *14*, 839-851.
2. Sailer, I.; Zembic, A.; Jung, R.E.; Hammerle, C.H.; Mattioli, A. Single-tooth implant reconstructions: Esthetic factors influencing the decision between titanium and zirconia abutments in anterior regions. *Eur. J. Esthet. Dent.* **2007**, *2*, 296-310.
3. Lughì, V.; Sergio, V. Low temperature degradation-aging-of zirconia: A critical review of the relevant aspects in dentistry. *Dent. Mater.* **2010**, *26*, 807-820.

4. Hisbergues, M.; Vendeville, S.; Vendeville, P. Zirconia: Established facts and perspectives for a biomaterial in dental implantology. *J. Biomed. Mater. Res. B Appl. Biomater.* **2009**, *88*, 519-529.
5. Kim, D.J.; Jung, H.J.; Jang, J.W.; Lee, H.L. Fracture toughness, ionic conductivity, and low-temperature phase stability of tetragonal zirconia codoped with yttria and niobium oxide. *J. Am. Ceram. Soc.* **1998**, *81*, 2309-2314.
6. Kim, D.J.; Lee, M.H.; Lee, D.Y.; Han, J.S. Mechanical properties, phase stability, and biocompatibility of (Y,Nb)-TZP/Ah03 composite abutments for dental implant. *J. Biomed. Mater. Res.* **2000**, *53*, 438-443.
7. Kim, D.J. Effect of Ta₂O₅, Nb₂O₅, and HfO₂ alloying on the transformability of Y₂O₃-stabilized tetragonal ZrO₂. *J. Am. Ceram. Soc.* **1990**, *73*, 115-120.
8. Cho, Y.D.; Shin, J.C.; Kim, H.L.; Gerelmaa, M.; Yoon, H.I.; Ryoo, H.M.; Kim, D.J.; Han, J.S. Comparison of the osteogenic potential of titanium and modified zirconia-based bioceramics. *Int. J. Mol. Sci.* **2014**, *15*, 4442-4452.
9. Cho, Y.D.; Hong, T.S.; Ryoo, H.M.; Kim, D.J.; Park, J.H.; Han, T.S. Osteogenic responses to zirconia with hydroxyapatite coating by aerosol deposition. *J. Dent. Res.* **2015**, *94*, 491-499.
10. Eisenbarth, E.; Meyle, J.; Nachtigall, W.; Breme, J. Influence of the surface structure of titanium materials on the adhesion of fibroblasts. *Biomaterials* **1996**, *17*, 1399-1403.
11. Zhao, B.; van der Mei, H.C.; Subbiahdoss, G.; de Vries, J.; Rustema-Abbing, M.; Kuijter, R.; Busscher, H.J.; Ren, Y. Soft tissue integration versus early biofilm formation on different dental implant materials. *Dent. Mater.* **2014**, *30*, 716-727.
12. Heydenrijk, K.; Meijer, H.J.; van der Reijden, W.A.; Raghoobar, G.M.; Vissink, A.; Stegenga, B. Microbiota around root-form endosseous implants: A review of the literature. *Int. J. Oral Maxillofac. Implant.* **2002**, *17*, 829-838.
13. Bruckmann, C.; Walboomers, X.F.; Matsuzaka, K.; Jansen, J.A. Periodontal ligament and gingival fibroblast adhesion to dentin-like textured surfaces. *Biomaterials* **2005**, *26*, 339-346.
14. Palaiologou, A.A.; Yukna, R.A.; Moses, R.; Lallier, T.E. Gingival, dermal, and periodontal ligament fibroblasts express different extracellular matrix receptors. *J. Periodontol.* **2001**, *72*, 798-807.
15. Quirynen, M.; De Soete, M.; Van Steenberghe, D. Infectious risks for oral implants: A review of the literature. *Clin. Oral Implant. Res.* **2002**, *13*, 1-19.
16. Koka, S. The implant-mucosal interface and its role in the long-term success of endosseous oral implants: A review of the literature. *Int. J. Prosthodont.* **1998**, *11*, 421-432.
17. Steinemann SG. Titanium-the material of choice? *Periodontol 2000* **1998**, *17*, 7-21.

18. Tete, S.; Mastrangelo, F.; Bianchi, A.; Zizzari, V.; Scarano, A. Collagen fiber orientation around machined titanium and zirconia dental implant necks: An animal study. *Int. J. Oral Maxillofac. Implant.* **2009**, *24*,52-58.
19. Oates, T.W.; Maller, S.C.; West, J.; Steffensen, B. Human gingival fibroblast integrin subunit expression on titanium implant surfaces. *J. Periodontol.* **2005**, *76*, 1743-1750.
20. Borghetti, P.; de Angelis, E.; Caldara, G.; Corradi, A.; Cacchioli, A.; Gabbi, C. Adaptive response of osteoblasts grown on a titanium surface: Morphology, cell proliferation and stress protein synthesis. *Vet. Res. Commun.* **2005**, *29*, 221-224.
21. Lincks, J.; Boyan, B.D.; Blanchard, C.R.; Lohmann, C.H.; Liu, Y.; Cochran, D.L.; Dean, D.D.; Schwiz, Z. Response of MG63 osteoblast-like cells to titanium and titanium alloy is dependent on surface roughness and composition. *Biomaterials* **1998**, *19*, 2219-2232.
22. Anselme, K.; Linez, P.; Bigerelle, M.; Le Maguer, D.; Le Maguer, A.; Hardouin, P.; Hildebrand, H.F.; lost, A.; Leroy, J.M. The relative influence of the topography and chemistry of TiAl₆V₄ surfaces on osteoblastic cell behaviour. *Biomaterials* **2000**, *21*, 1567-1577.
23. Cochran, D.L.; Simpson, J.; Weber, H.P.; Buser, D. Attachment and growth of periodontal cells on smooth and rough titanium. *Int. J. Oral Maxillofac. Implant.* **1994**, *9*,289-297
24. Bachle, M.; Kohal, R.J. A systematic review of the influence of different titanium surfaces on proliferation, differentiation and protein synthesis of osteoblast-like MG63 cells. *Clin. Oral Implant. Res.* **2004**, *15*, 683-692.
25. Chehroudi, B.T.R.L.; Gould, T.R.L.; Brunette, D.M. Titanium-coated micromachined grooves of different dimensions affect epithelial and connective-tissue cells differently *in vivo*. *J. Biomed. Mater. Res.* **1990**, *24*, 1203-1219.
26. Yamano, S.; Ma, A.K.; Shanti, R.M.; Kim, S.W.; Wada, K.; Sukotjo, C. The influence of different implant materials on human gingival fibroblast morphology, proliferation, and gene expression. *Int. J. Oral Maxillofac. Implant.* **2011**, *26*,1247-1255.
27. Kim, H.; Murakami, H.; Chehroudi, B.; Textor, M.; Brunette, D.M. Effects of surface topography on the connective tissue attachment to subcutaneous implants. *Int. J. Oral Maxillofac. Implant.* **2006**, *21*,354-365.
28. Brunette, D.M.; Chehroudi, B. The effects of the surface topography of micromachined titanium substrata on cell behavior *in vitro* and *in vivo*. *J. Biomech. Eng.* **1999**,*121*,49-57.
29. Mustafa, K.; Oden, A.; Wennerberg, A.; Hultenby, K.; Arvidson, K. The influence of surface topography of ceramic abutments on the attachment and proliferation of human oral fibroblasts. *Biomaterials* **2005**, *26*, 373-381.
30. Mustafa, K.; Wroblewski, J.; Lopez, B.S.; Wennerberg, A.; Hultenby, K.; Arvidson, K.

- Determining optimal surface roughness of TiO₂ blasted titanium implant material for attachment, proliferation and differentiation of cells derived from human mandibular alveolar bone. *Clin. Oral Implant. Res.* **2001**, *12*, 515-525.
31. Borsani, E.; Salgarello, S.; Mensi, M.; Boninsegna, R.; Stacchiotti, A.; Rezzani, R.; Sapelli, P.; Bianchi, R.; Rodella, L.F. Histochemical and immunohistochemical evaluation of gingival collagen and metalloproteinases in peri-implantitis. *Acta Histochem.* **2005**, *107*, 231-240.
 32. Humphries, J.D.; Byron, A.; Humphries, M.J. Integrin ligands at a glance. *J. Cell Sci.* **2006**, *119*, 3901-3903.
 33. Pivodova, V.; Frankova, J.; Ulrichova, J. Osteoblast and gingival fibroblast markers in dental implant studies. *Biomed. Pap. Med. Fae. Univ. Palacky Olomouc Czech. Repub.* **2011**, *155*, 109-116.
 34. Hynes, R.O. Integrins: Versatility, modulation, and signaling in cell adhesion. *Cell* **1992**, *69*, 11-25.
 35. Humphries, M.J. Integrin structure. *Biochem. Soc. Trans.* **2000**, *28*, 311-339.
 36. Hormia, M.; Ylanne, J.; Virtanen, I. Expression of integrins in human gingiva. *J. Dent. Res.* **1990**, *69*, 1817-1823.
 37. Geiger, B.; Bershadsky, A.; Pankov, R.; Yamada, K.M. Transmembrane crosstalk between the extracellular matrix and the cytoskeleton. *Nat. Rev. Mol. Cell Biol.* **2001**, *2*, 793-805.
 38. Riikonen, T.; Westermarck, J.; Koivisto, L.; Broberg, A.; Kahari, V.M.; Heino, J. Integrin $\alpha 2\beta 1$ is a positive regulator of collagenase (MMP-1) and collagen $\alpha 1$ (I) gene expression. *J. Biol. Chem.* **1995**, *270*, 13548-13552.
 39. Pae, A.; Lee, H.; Kim, H.S.; Kwon, Y.D.; Woo, Y.H. Attachment and growth behavior of human gingival fibroblasts on titanium and zirconia ceramic surfaces. *Biomed. Mater.* **2009**, *4*.

국문초록

(Y, Nb)-zirconia의 골형성능과 치은세포 반응에 관한 연구

서울대학교 대학원 치의과학과 치과보철학 전공

(지도교수 한 중 석)

신 지 철

1. 목적

심미성을 고려한 임플란트 재료로 최근 3Y-TZP 지르코니아가 사용되고 있으나 기능이 가해지면서 체액과 접촉하는 골내 임플란트 재료로 사용하면 저온열화(low temperature degradation)가 발생할 가능성이 높아 안정성을 해칠 수 있다. 이러한 현상을 해결하기 위해 지르코니아에 yttrium oxide와 tantalum oxide 또는 yttrium oxide와 niobium oxide를 혼합하여 저온열화를 제어한 tetragonal zirconia polycrystals이 개발되었다. 새롭게 개발된 modified zirconia가 임상에서 임플란트로 사용가능한지 여부를 평가하기 위하여 골형성능을 기존의 타이타늄과 비교하고, 주변 연조직과의 반응도 평가하기 위하여 human gingival fibroblasts (HGFs)에 대한 생체적합성을 평가하였다.

2. 방법

골형성능 연구에서는 Titanium-machined, Titanium-anodizing, sandblasted (Y, Ta)-TZP, sandblasted (Y, Nb)-TZP 표면을 confocal laser microscopy와 SEM으로 관찰하였다. 각각의 표면에 mouse pre-osteoblast cell을 배양한 후, cell attachment와 morphology는 confocal laser microscopy로 관찰하고 cellular proliferation은 PicoGreen assay로 평가하였으며, osteoblast differentiation은 real-time PCR로 확인하였다.

치은세포반응 연구에서는 Titanium-machined, Ti-anodizing, polished (Y, Nb)-TZP, sandblasted (Y, Nb)-TZP의 surface roughness와 topography를 3-D confocal laser microscope로, surface morphology를 SEM으로 관찰하였다. Human gingival fibroblast를 각 시편 표면에 배양한 후 cell attachment와 morphology는 confocal laser microscopy로 관찰하고 cell proliferation은 PicoGreen assay로 평가하였으며, cell differentiation은 real time PCR로 확인하였다.

3. 결과

표면 거칠기에 상관없이 조골모세포가 지르코니아 표면에 타이타늄 표면만큼 효율적으로 부착했다. 거친 표면보다는 연마된 표면에 세포증식이 잘 되었지만 골형성 반응에서는 거친 표면이 우세하였다. (Y, Ta)-TZP와 (Y, Nb)-TZP 표면의 세포는 anodized titanium 표면의 경우와 유사한 증식능력을 보였다. (Y, Ta)-TZP와 (Y, Nb)-TZP 표면의 조골모세포의 골형성능은 rough-surface titanium 표면의 경우와 유사하였다.

polished (Y, Nb)-TZP 표면에 배양된 HGFs는 6시간 후 rounded cell morphology와 light spreading을 보이다가 7일 후에 증식률이 다른 표면들의 경우보다 뚜렷하게 높아졌다. 같

은 표면에서 type I collagen, integrin $\alpha 2$ 과 $\beta 1$ 의 mRNA expression은 24시간 후 뚜렷하게 활성화되었다.

4. 결론

(Y, Nb)-TZP는 fixture level에서는 골유착에 적절한 표면 상태를 제공하고 abutment level에서는 peri-implant mucosal sealing에 적절한 표면을 제공함으로써 임상적으로 유용한 임플란트 재료로서의 성질을 갖추었다.

주요어: dental implant, titanium, zirconia, LTD, niobium, osteogenic potential, human gingival fibroblasts (HGFs), mucosal sealing

